Electrochemical and Solid-State Letters, **10** (7) K20-K23 (2007)
1099-0062/2007/10(7)/K20/4/$20.00 © The Electrochemical Society

Photoluminescence Study of an Er-Doped Si-Rich SiO_x Film

Effects of Annealing Gas Ambients and Double-Step Processes

C. L. Heng,* O. H. Y. Zalloum, T. Roschuk, D. Blakie, J. Wojcik, and P. Mascher*,z**

Department of Engineering Physics and Centre for Emerging Device Technologies, McMaster University, Hamilton, Ontario L8S 4K1, Canada

We have studied photoluminescence (PL) from samples of Er-doped Si-rich silicon oxide (SRSO) annealed at 875°C for 1 h in N_2, N_2 + 5% H_2 (FG1), Ar + 5% H_2 (FG2), and O_2, respectively, or subjected to double-step annealing processes. For the given film composition, the PL spectra of the samples annealed in N_2, FG1, or FG2 are similar in shape but reveal small differences in the intensities of emission bands; while the spectra are qualitatively different in the case of oxidation. By combining the treatments of oxidation and annealing in FG1, the PL intensity of the SRSO matrix increases significantly; the emission from Si nanoclusters (Si-ncls) is also enhanced while the Er^{3+} 1.54 μm PL remains efficient. The effects of annealing gas ambients are discussed in terms of hydrogen passivation, Si oxynitridation and/or oxidation occurring in the film upon annealing and play different roles in the PL.
© 2007 The Electrochemical Society. [DOI: 10.1149/1.2735815] All rights reserved.

Manuscript submitted February 8, 2007; revised manuscript received March 9, 2007. Available electronically May 2, 2007.

Er-doped Si-rich Si oxide (SRSO) has been studied intensively for the development of light sources or optical amplifiers at ~1.54 μm in telecommunications, as well as the red, green, and blue for display applications.[1] A major driving force behind the development is the requirement for a wide range of low-cost and compact optical components for implementation of wavelength-division multiplexing (WDM) in fiber-to-the-home systems.[2] The Er^{3+} photoluminescence (PL) is believed to occur mainly through the recombination of photogenerated excitons within Si nanoclusters (Si-ncls) which transfer their energy to the nearby Er^{3+} ions. Amorphous Si-ncls as well as Si nanocrystals have been demonstrated to be effective sensitizers for the Er PL.[3] The coupling between luminescent centers (Si-ncls and defects) in the SRSO matrix and the Er dopant usually produces an overall quenching of the intrinsic PL from these centers, although undoped SRSO has been shown to be an efficient luminescent material and has wide applications in optoelectronics.[4,5] The PL from the SRSO matrix is mainly related to the Si-ncls and defects and depends strongly on the annealing conditions under which they are formed. In an Er-doped SRSO film containing Si-ncls, the Er PL depends on the efficiency of energy transfer from Si-ncls to Er^{3+} ions. The energy-transfer efficiency decreases as the separation distance between the Si-ncls and Er^{3+} ions increases.[6-8] Oxidation can reduce the effective size of Si-ncls by converting the material of the outer layer of the nanoclusters into Si oxide that can contain PL-emitting defects. Accordingly, the resultant oxide can reduce the efficiency of energy transfer from Si-ncls to Er ions and hence decreases the Er emission.

The room-temperature oxidation of Si-ncls in porous Si matrix has been investigated by Wolkin et al.[9] The Si═O bonds are believed to form at the SiO_2/Si-ncl interface, which plays a crucial role to the electronic states and PL of Si-ncls with size less than 3 nm. Pi et al.[10] studied the formation and oxidation of Si-ncls in the Er-doped SRSO films and gave a kinetic model for the cluster formation and oxidation. Moreover, Wilkinson and Elliman[11] reported effects of annealing ambients [Ar, N_2, or N_2 + 5% H_2 (FG1)] on the luminescence from Si nanocrystals in silica and ascribed the effects to variations in nanocrystal size and defect states at the Si nanocrystal/oxide interface. Comedi et al.[12] found that the long wavelengths in Si-ncls-related PL spectra are preferably enhanced by annealing of the SRSO films in an Ar + 5% H_2 (FG2) ambient. Here, we study the PL from an Er-doped SRSO film annealed in various gas ambients in both single- and double-step processes. We demonstrate that the PL from the SRSO matrix can be significantly enhanced, while the Er^{3+} PL remains efficient for the given film composition.

Experimental

The Er-doped SRSO film was synthesized on a single-crystal Si substrate by electron cyclotron resonance plasma-enhanced chemical vapor deposition using SiH_4 and O_2 as precursors, with in situ Er doping using a volatile metallorganic Er source. The deposition system has been described in detail elsewhere.[13] The thickness of the film was about 56 nm measured by transmission electron microscopy (TEM). Rutherford backscattering spectroscopy (RBS) analysis shows that the Si concentration in the film is 44.7 atom % with an Er concentration of 1.2 atom %. The film with the substrate was then cleaved into small pieces and annealed at 875°C in the gas ambients of N_2, FG1, FG2, or O_2 for 1 h or subjected to double-step processes as described in the text. Energy-filtered TEM (EFTEM) was used to study the precipitation of Si-ncls in the film. The microscope used was a JEOL 2010F field-emission gun transmission electron microscope operating at 200 kV.

The PL was excited with an unfocused beam (~1 mm diam) using the 325 nm line of a He–Cd laser with a nominal power of 17 mW. The PL spectra in the 1400–1700 nm range were measured using a 500 mm grating monochromator (3 mm slits), a lock-in amplifier with a chopper working at 40 Hz, and an InGaAs detector. The system response curve for the monochromator is flat over the bandwidth of the Er signal near 1540 nm and therefore, the spectra do not require further correction. The PL spectra in the 350–850 nm range were measured using a charge-coupled device (CCD)-based spectrometer. These PL spectra were corrected for system response and optics transmission and subsequently converted to, and presented in, normalized photon flux (arbitrary units). A full description of the CCD-based PL system and the data correction methodology is given elsewhere.[14] All the measurements were performed at room temperature.

Results and Discussion

The Er^{3+} 1.54 μm PL from the film is most intense after annealing the film at 875°C in flowing N_2 for 30 min. Figure 1 shows an EFTEM image and reveals the precipitation of Si-ncls in such an annealed film. The image was taken using a 3 eV slit in the Si plasmon region (16–19 eV). The white dots with sizes of about 3–4 nm are Si-ncls in the SRSO matrix. The average size is a little larger than that reported by Iacona et al. in a SRSO film with similar Si concentration.[15] This suggests that Er doping is beneficial to the nucleation and growth of Si clusters. Note that there is a layer approximately 15 nm in thickness (denoted by an arrow) which shows

* Electrochemical Society Active Member.
** Electrochemical Society Student Member.
z E-mail: mascher@mcmaster.ca

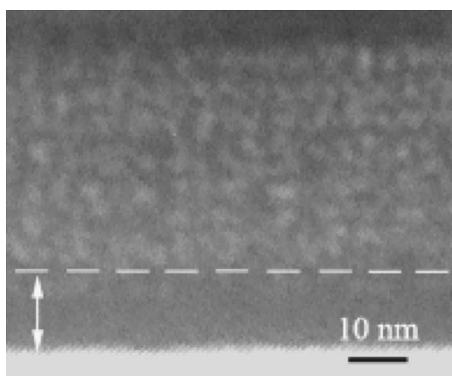

Figure 1. EFTEM image of the film after annealing at 875°C in N_2 for 30 min.

almost no Si grains. This could be due to redistribution of the excess Si and/or the Si diffusing toward the interface between the film and the substrate upon annealing.

Figures 2a and b show PL spectra of the samples annealed at 875°C for 1 h in N_2, FG1, FG2, or O_2. In Fig. 2a, the spectra are in a range of 350–850 nm, indicating visible emission from the SRSO matrix of the film. For the sample annealed in N_2, there are four main emission bands in the spectrum located at approximately 440, 550, 660, and 800 nm. After annealing in FG1 or FG2, the PL spectra are similar in shape to the case of annealing in N_2, but the emission bands in each PL spectrum have small differences in intensity. Among the three gas ambients, annealing in FG2 yields the strongest PL spectrum; the 440 nm band has the lowest intensity after the FG1 annealing, while the 660 and 800 nm bands are lowest after the N_2 annealing. However, the PL spectrum of the sample annealed in O_2 is quite different: a ~405 nm band emerges and becomes the dominant peak, while the 440 nm band is also present but as a shoulder. The 660 nm emission band, which can be ascribed to nonbridging oxygen hole centers (NBOHC) in SiO_2,[16] is weaker than in the cases of annealing in the other three gas ambients. The 440 nm band likely is from oxygen deficiency centers (ODCs) which are often considered to be the origin of short-wavelength PL in the SRSO films.[17] The 550 nm peak originates from transitions from the Er^{3+}-excited states to the ground state ($^4S_{3/2} \rightarrow {}^4I_{15/2}$),[1] while the 800 nm emission should result from radiative recombination within the Si-ncls. For the origin of the 405 nm band, Chen et al.[18] have attributed an emission band in the range of 405–416 nm to localized surface states at the SiO_x/Si interface after oxidation of Si nanocrystals. Here, we suggest that the localized surface states could be weak oxygen bonds (WOBs). Even though no interstitial O atoms are generated as through Si implantation,[19] the O atoms in our case can be incorporated from the annealing ambient into the film upon oxidation as suggested by Pi et al.[10]

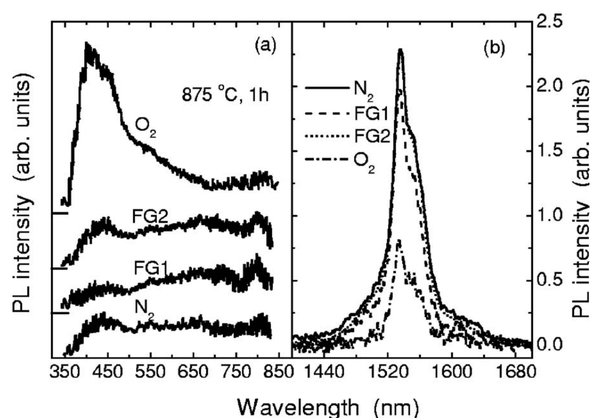

Figure 2. (a) PL spectra in the range of 350–850 nm for the film annealed at 875°C for 1 h in gas ambients of N_2, FG1, FG2, or O_2 and (b) the Er^{3+} 1.54 μm PL from the film after the above gas ambients annealing.

The Er^{3+} 1.54 μm PL spectra for the samples after annealing in the above gas ambients are shown in Fig. 2b. Annealing the sample in N_2 yields the highest Er PL intensity. The intensity is nearly identical in the case of FG2 annealing but decreases by ~10% when annealed in FG1 and decreases by ~63% after oxidation. Note that the full widths at half-maximum (fwhms) of the spectra are also different. The fwhm of the spectrum in the case of N_2 annealing is ~40 nm; the width decreases slightly to 37 nm after annealing in FG1 (or FG2) but reduces further to 29 nm after the 875°C oxidation. Such variations in the PL intensities and the fwhms reflect different chemical reactions occurring in the film under each anneal ambient. Each emission band is affected differently. Because H_2 is the only reactive species in the FG2 ambient, H_2 passivation of nonradiative recombination in the film explains the enhancement of the PL spectrum, especially at longer wavelengths.[20] N_2 is believed to be relatively inert for annealing temperatures less than 1200°C; direct nitridation of Si in pure N_2 requires temperatures in the 1200–1300°C range due to the high strength of the N≡N bond (9.8 eV/molecule);[21] but N can incorporate at the interface of Si/SiO_2 during high-temperature annealing,[22] and N_2 has been reported to react with Si at moderate temperatures (760–1050°C) in the presence of gas-phase impurities (H_2, O_2, CO_2) to form ultrathin (<1.2 nm) oxynitride films near the interface.[23] The differences in the intensities of the 440 nm band among the cases of annealing in N_2, FG1, or FG2, suggest that annealing in FG1 has decreased the amount of ODC defects, and possibly formed a very thin Si oxynitride layer at the surface of Si-ncls. The Si oxynitride is reported to have an emission wavelength at ~430 nm,[24] but the amount of the oxynitride may be so small that it does not exhibit an obvious emission band. If this is the case, then one may propose that the oxynitride should also be responsible for the small decrease of Er PL by hindering slightly the energy transfer from the Si-ncls to nearby Er^{3+}; while the much stronger decrease after the oxidation is believed to be due to less formation of Si-ncls and/or due to a decrease in effective Si-ncl size.[10]

Figures 3a-f show the PL spectra for the range 350–850 nm after subjecting the samples to different double-step annealing processes in the gas ambients indicated. For the samples annealed at 875°C for 1 h in N_2, FG1, or FG2, the effects of a secondary oxidation for 1 h at 850°C are shown in Fig. 3a-c. After annealing in N_2 or FG2 and then in O_2 (Fig. 3a and c), the shapes of the PL spectra are similar to the cases of annealing in N_2 (or FG2) alone; however, the intensities are observed to be ~10–20% higher than in the latter cases. After annealing in FG1 and then in O_2 (Fig. 3b), the main peak of the spectrum has shifted to ~400 nm and its intensity increased about 9 times that for the case of annealing only in FG1. The significant increase of the PL intensity should be related to the introduction of defects (possibly Si oxynitride and WOB) upon double-step annealing: the Si oxynitride forms upon the FG1 annealing, then many more WOB defects form after the secondary oxidation, and hence the peak position of the spectrum exhibits the small blue-shift.

For the samples initially oxidized at 875°C for 1 h, again, the PL spectra are quite different after secondary annealing at 875°C for 1 h in either N_2, FG1, or FG2, as shown in Fig. 3d-f. In Fig. 3d and f, the intensities of PL bands in the blue region of the spectra are 10–20% lower than in the case of oxidation alone; the emission at longer wavelengths for secondary annealing in N_2 (Fig. 3d) is similar to the case of oxidation alone (Fig. 2a), while the 660 nm band is more pronounced in FG2 secondary annealing. For secondary annealing in FG1 (Fig. 3e), the PL intensity of the blue band is 25% more intense than in the case of oxidation alone; additionally, the 660, and especially the 820 nm band are observed to be more enhanced. The increase of the PL intensity of the blue band could be

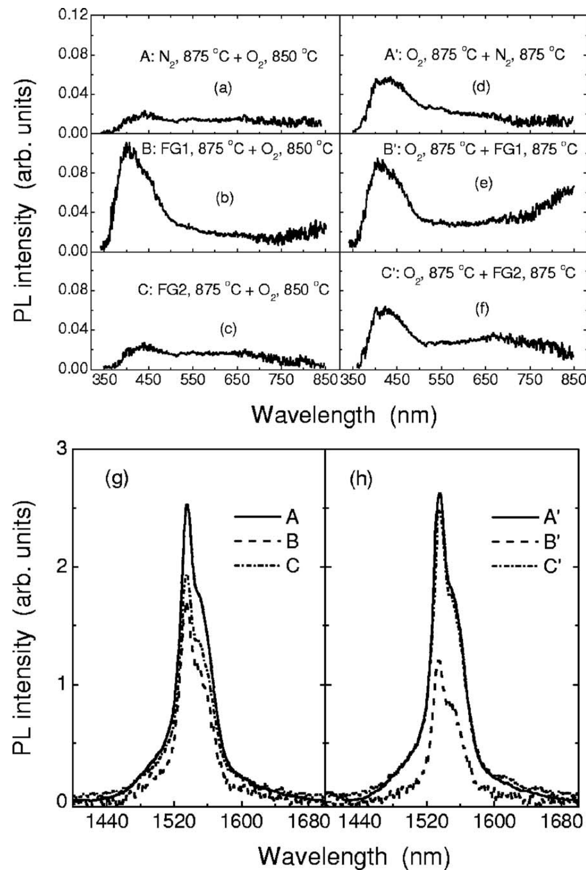

Figure 3. (a–c) PL spectra in the range of 350–850 nm for the samples annealed at 875°C for 1 h in N_2, FG1, or FG2 and then oxidized at 850°C for 1 h (A, B, and C), and for the samples initially oxidized at 875°C for 1 h and then annealed at 875°C for 1 h in N_2, FG1, or FG2 (A′, B′, and C′); (g and h) Er^{3+} 1.54 μm PL for the film after the above double-step processes.

due to additional Si oxynitride formation, with its luminescence superimposing onto the emission band resulting from the WOB defects. The fact that the 660 nm band is more evident after the secondary FG1 (or FG2) annealing is likely due to the H_2 passivation being beneficial to the formation of NBOHC, possibly by breaking the weak O–O bonds. If so, this indicates that the precursor of the NBOHC could be WOB in our film.[19,25] The enhanced emission band near 820 nm after annealing in O_2 followed by secondary annealing in FG1 (Fig. 3e), is believed to be due to the enhanced radiative recombination within the Si-ncls in the prevalence of Si oxynitride near the surface of Si-ncls, which hinders the energy transfer from Si-ncls to Er^{3+}.

Figures 3g and h show the Er^{3+} 1.54 μm PL spectra for the samples after the above-described double-step annealing processes. When compared to the cases of annealing in N_2, FG1, or FG2 alone (Fig. 2b), the Er PL intensity after the secondary oxidation (Fig. 3g) has increased by 10% for the case of initial annealing in N_2, while both intensities decreased by ~14% for the cases of initial annealing in FG1 (or FG2). The mentioned 10% increase of the Er PL intensity is believed to be mainly due to slightly more Si-ncls formed in the film than in the case of annealing in N_2 alone, while the decrease is likely related to the Si oxide and/or oxynitride formation at the surface of the Si-ncls, which partly hinders the energy transfer. Note also that the Er PL intensities are each comparable to the cases without the secondary oxidation. This indicates that the oxidation of Si-ncls at 850°C should be small or the cluster oxidation is a self-limiting process as in the Si nanocrystal case.[18,26] Compared to the case of oxidation alone, the Er PL intensity of the spectrum for the sample initially oxidized has increased by 50% after secondary annealing in FG1 and increases about two times after secondary annealing in N_2 (or FG2), as shown in Fig. 3h. The pronounced enhancements of the Er PL intensity mean that either the number of active Si-ncls and/or the effective Si-ncl size[10] increased.

Based on the above results, it can be seen that by combining the treatments of annealing in FG1 and oxidation, the PL from the SRSO matrix can be greatly enhanced; the luminescence from Si-ncls can also be controlled by exchanging the annealing and oxidation order, while the Er PL remains efficient after the double-step annealing processes. However, the annealing effects from the gas ambients are closely related to the concentration of both Si and Er inside the Er-doped SRSO films.[27]

Conclusions

We have studied the PL spectra of an Er-doped SRSO film annealed under various conditions. The differences in the PL spectra after annealing the film in N_2, FG1, FG2, or O_2 likely are related to hydrogen passivation and Si oxynitride and/or Si oxide formation at the surface of Si-ncls. By combining the treatments of annealing in FG1 and oxidation or vice versa, the defects PL from the SRSO matrix of the film increases significantly. The enhancement of the 660 nm band indicates that H_2 passivation is beneficial to the formation of NBOHC, and the precursor of the NBOHC could be WOB. This study is important to enhancing the understanding of the sensitivity of PL to annealing ambient in Er-doped thin films.

Acknowledgments

The authors wish to acknowledge valuable technical support by Jim Garrett during annealing experiments, as well as Dr. Carmen Andrei and Mr. Fred Pearson in TEM observation. We also gratefully acknowledge Professor W. Lennard for RBS measurements. This work has been supported by the Ontario Research and Development Challenge Fund under the auspices of the Ontario Photonics Consortium.

McMaster University assisted in meeting the publication costs of this article.

References

1. A. Polman, *J. Appl. Phys.*, **82**, 1 (1997).
2. A. J. Kenyon, C. E. Chryssou, C. W. Pitt, T. Shimizu-Iwayama, D. E. Hole, N. Sharma, and C. J. Humphreys, *J. Appl. Phys.*, **91**, 367 (2002).
3. G. Franzò, S. Boninelli, D. Pacifici, F. Priolo, F. Iacona, and C. Bongiorno, *Appl. Phys. Lett.*, **82**, 3871 (2003).
4. *Silicon Photonics*, L. Pavesi and D. J. Lockwood, Editors, Springer, Berlin (2004).
5. R. J. Walters, G. I. Bourianoff, and H. A. Atwater, *Nat. Mater.*, **4**, 143 (2005).
6. T. Kimura, H. Isshiki, S. Ide, T. Shimizu, and T. Ishida, *J. Appl. Phys.*, **93**, 2595 (2003).
7. J. H. Jhe, J. H. Shin, K. J. Kim, and D. W. Moon, *Appl. Phys. Lett.*, **82**, 4489 (2003).
8. V. Yu. Timoshenko, M. G. Lisachenko, O. A. Shalygina, B. V. Kamenev, D. M. Zhigunov, S. A. Teterukov, P. K. Kashkarov, J. Heitmann, M. Schmidt, and M. Zacharias, *J. Appl. Phys.*, **96**, 2254 (2004).
9. M. V. Wolkin, J. Jorne, P. M. Fauchet, G. Allan, and C. Delerue, *Phys. Rev. Lett.*, **82**, 197 (1998).
10. X. D. Pi, O. H. Y. Zalloum, J. Wojcik, A. P. Knights, P. Mascher, A. D. W. Todd, and P. J. Simpson, *J. Appl. Phys.*, **97**, 096108 (2005).
11. A. R. Wilkinson and R. G. Elliman, *J. Appl. Phys.*, **96**, 4018 (2004).
12. D. Comedi, O. H. Y. Zalloum, and P. Mascher, *Appl. Phys. Lett.*, **87**, 213110 (2005).
13. M. Boudreau, M. Boumerzoug, P. Mascher, and P. E. Jessop, *Appl. Phys. Lett.*, **63**, 3014 (1993).
14. O. H. Y. Zalloum, M. Flynn, T. Roschuk, J. Wojcik, E. Irving, and P. Mascher, *Rev. Sci. Instrum.*, **77**, 023907 (2006).
15. F. Iacona, C. Bongiorno, C. Spinella, S. Boninelli, and F. Priolo, *J. Appl. Phys.*, **95**, 3723 (2004).
16. L. N. Skuja and A. R. Silin, *Phys. Status Solidi A*, **56**, K11 (1979).
17. L. Rebohle, J. von Borany, H. Fröb, and W. Skorupa, *Appl. Phys. B*, **71**, 131 (2000).
18. X. Y. Chen, Y. F. Lu, Y. H. Wu, B. J. Cho, M. H. Liu, D. Y. Dai, and W. D. Song, *J. Appl. Phys.*, **93**, 6311 (2003).
19. G.-R. Lin, C.-J. Lin, C.-K. Lin, L.-J. Chou, and Y.-L. Chueh, *J. Appl. Phys.*, **97**, 094306 (2005).
20. D. Comedi, O. H. Y. Zalloum, E. A. Irving, J. Wojcik, and P. Mascher, *J. Vac. Sci. Technol. A*, **24**, 817 (2006).
21. S. K. Ghandi, *VLSI Fabrication Principles: Silicon and Gallium Arsenide*, 2nd ed.,

Wiley, New York (1994).
22. S. I. Raider, R. A. Gdula, and J. R. Petrak, *Appl. Phys. Lett.*, **27**, 150 (1975).
23. A M. L. Green, T. Sorsch, L. C. Feldman, W. N. Lennard, E. P. Gusev, E. Garfunkel, H. C. Lu, and T. Gustafsson, *Appl. Phys. Lett.*, **71**, 2978 (1997).
24. J. Zhao, Y. H. Yu, D. S. Mao, Z. X. Lin, B. Y. Jiang, G. Q. Yang, X. H. Liu, and S. Zou, *Nucl. Instrum. Methods Phys. Res. B*, **148**, 1002 (1999).
25. H. Nishikawa, R. Nakamura, R. Tohmon, Y. Ohki, Y. Sakurai, K. Nagasawa, and Y. Hama, *Phys. Rev. B*, **41**, 7828 (1990).
26. D. B. Kao, J. P. McVittie, W. D. Nix, and K. C. Saraswat, *IEEE Trans. Electron Devices*, **ED-35**, 25 (1988).
27. D. E. Blakie, O. H. Y. Zalloum, J. Wojcik, E. A. Irving, A. P. Knights, and P. Mascher, *Appl. Phys. Lett.*, Submitted.